



# Fast microwave synthesis of high-silica natural soil based porous geopolymer

Naritsara TOOBPENG<sup>1</sup>, and Sirithan JIEMSIRILERS<sup>1,\*</sup>

<sup>1</sup> Chulalongkorn University, Upcycled Materials from Industrial and Agricultural Wastes Research Unit, Department of Materials Science, Faculty of Science, Bangkok 10330, Thailand

\*Corresponding author e-mail: sirithan.j@chula.ac.th

**Received date:**

31 August 2023

**Revised date**

12 January 2024

**Accepted date:**

18 February 2024

**Keywords:**

Geopolymer;  
Soil;  
Porous;  
Microwave;  
Silica

**Abstract**

This study describes a simple microwave process for fabricating porous geopolymer-polymer based Shirasu soil. The porous geopolymer samples were synthesized using sodium silicate ( $\text{Na}_2\text{SiO}_3$ ) and sodium hydroxide (NaOH) solution as alkaline solution in range of 0.5 M to 9 M. After mixing process, the geopolymer slurry was heated and stimulated geopolymerization reaction by different microwave powers at 200 W, 500 W and 700 W for 30 s, 60 s, 90 s and 120 s. The influence of NaOH concentration, microwave powers and heating times on the apparent bulk density, the water adsorption was focused. Results showed that the microwave powers and heating time affected the apparent bulk density, the water adsorption, and the densification of geopolymer matrix. Higher microwave power can promote higher water adsorption related to lower apparent bulk density. Moreover, the results revealed that the porosity and the nitrogen adsorption of geopolymers at 120 s of heating time increased with an increment of the NaOH from 1 M to 4 M. On the other hand, geopolymers activated by 200 W at 30 s could not be hardened. This work provides the feasibility of porous geopolymer synthesis based natural soil.

## 1. Introduction

Geopolymer technology has been developed as a feasible alternative for cement manufacturing due to its excellent mechanical properties and eco-friendly processes with a dramatic reduction of greenhouse emissions. Basically, geopolymer material can be synthesized based on the reaction of aluminosilicate precursor and high alkali-activating agent. The alkaline agent can be prepared by modifying soluble silicate with a high alkaline solution. The geopolymerization is exothermic reaction and starts with an initial dissolution step following by condensation reaction [1-3]. In theory, the whole aluminosilicate precursor could be formed as an amorphous three-dimensional aluminosilicate structure with a practical formula of  $M_n[-(\text{SiO}_2)_z-\text{AlO}_2]_n \cdot x\text{H}_2\text{O}$ , where x is the water content, z is the molar ratio of Si to Al, M is an alkali cation and n is the degree of polymerization [4]. Although geopolymer materials have been admired in recent years due to their excellent mechanical properties and disabilities in severe environments, their synthesis requires large amounts of alkaline activator and also need curing time for mechanical properties development.

There are various aluminosilicate compounds that can be used to synthesize geopolymer materials, such as calcined clays and industrial wastes. When any aluminosilicate precursors are dissolved with alkali activators, the inorganic geopolymer materials are formed [5,6]. Several industrial wastes are used as aluminosilicate precursors, such as metakaolin, fly ash and calcined clay. Apart from those, in recent years, Shirasu natural pozzolan was considered as partial replacement of concrete because of its strength and aggressive chemical resistance. However, the soil has not been studied in geopolymer

materials yet. Therefore, it is interesting to utilize Shirasu natural soil as an aluminosilicate for geopolymer synthesis.

Owing to the Sustainable Development Goals (SDGs) perspective following green environmental concept, geopolymer synthesis has been altered and applied by many researchers. To date, researchers have explored several methods for the synthesis and preparation of porous geopolymers. Generally, the methods can be divided into four processes following: (1) direct foaming, (2) additive manufacturing, (3) sacrificial template, (4) fast microwave foaming or a combination of the above methods base on their use to various practical applications [35]. The typical direct foaming technique is widely used in lightweight concrete and porous ceramics fabrication. Previous research prepared porous geopolymer using direct foaming process by adding additives. Fresh geopolymer foam is produced and then gas products occur under slightly increase temperature [36]. For sacrificial template method, the porous geopolymer is prepared by mixing with an amount of a sacrificial template filler, generally polylactic acid (PLA), and then eliminates the filler to form a porous geopolymer by heat treatments [37]. Moreover, the additive manufacturing method is also a method to produce porous materials by adding additives to prepare complex geopolymer structures which controllable pore size and pore distribution. The different additives are used in all above methods. On the other hand, for fast microwave foaming method, there is no requirement to add the additives, but the porous geopolymers usually can be cured under microwave radiation with a shorter curing time. The benefits of microwave heating are instantaneous, very rapid heating and easy control. Another advantage is that the microwave energy is directly transferred to the material at the water molecule level, subsequently

the water in the entire body suddenly reaches a higher temperature and generates a foam structure [38].

Recently, Onutai *et al.* [7] has been developed porous geopolymer synthesis by applying microwave energy to stimulate geopolymerization reaction and to reduce curing time. Microwave heating under electromagnetic conversion involves the electromagnetic energy to thermal energy [8]. This energy can accelerate the geopolymerization and enhance the temperature of material. Moreover, higher microwave power can provide the strength development of porous geopolymers based fly ash at early stage [9]. Additionally, microwave technique can rapidly stimulate geopolymerization reaction by removal of water content results in porosity occurrence [10]. On the other hand, the conventional curing process requires a long heating period in an oven to obtain strength development. Up to now, porous geopolymer has been adapted in various applications. Huan Gao *et al.*, [11] applied porous geopolymer in building thermal insulation. Moreover, pyrophyllite clay based porous geopolymers was studied and used for removal of methylene blue from aqueous solutions [12,13]. Industrial wastewater containing heavy metals was also adsorbed by steel slag-based porous geopolymer for copper and lead removal because of mesoporous geopolymer material [14,15]. Additionally, Yanli Wang *et al.*, [16] showed the excellent CO<sub>2</sub> adsorption capacity of amine functionalized porous geopolymer and provided a new method for the resource utilization of fly ash.

As mentioned above, although a fast microwave method was proposed for porous geopolymer synthesis, the Shirasu natural soil synthesized by fast microwave method has not been studied yet and its performance to be synthesized as porous geopolymer is still unclear. This paper investigates the feasibility of porous geopolymer synthesis based Shirasu soil using microwave radiation. Moreover, a comparison on microwave power and its effect on bulk density and water absorption are also explored.

## 2. Experimental

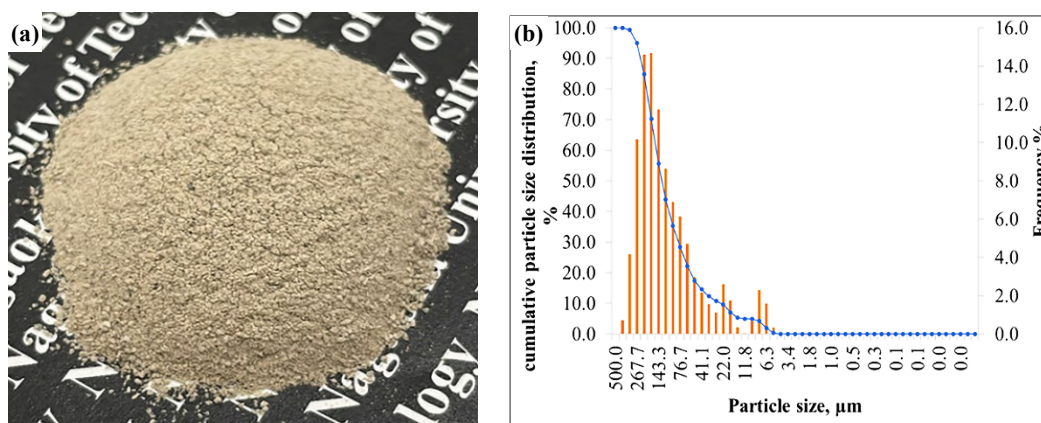


Figure 1. The appearance (a), and the cumulative particle size distribution (b) of Shirasu soil.

Table 1. Chemical composition of Shirasu soil (by weight).

Oxide	Al <sub>2</sub> O <sub>3</sub>	Fe <sub>2</sub> O <sub>3</sub>	SiO <sub>2</sub>	CaO	MgO	Na <sub>2</sub> O	K <sub>2</sub> O	Others
wt%	13.50	2.62	68.90	1.94	0.33	2.90	4.30	5.51

## 2.1 Material

Natural soil obtained from Shirasu-Daichi; Japan was used as an aluminosilicate source material for porous geopolymer synthesis. The original soil was dried, sieved through a 35 mesh, and then bagged for mineral and chemical characterization. Figure 1 displays the appearance and the cumulative particle size distribution of the soil. As seen in Figure 1(a), the soil exhibits brownish color. Shirasu is one of the unused natural resources and a deposit richly available in the southern part of Kyushu Island. It has a large amount of very fine particles with ranges of density from 2.1 g·cm<sup>-3</sup> to 2.7 g·cm<sup>-3</sup> [17]. The particle diameters of the soil, D10, D50 and D90, were 23.4 μm, 129.7 μm and 241.3 μm, respectively as shown in Figure 1(b). The mineral composition of the soil analyzed by XRD analysis is displayed in Figure 2. Based on XRD result, it was found the crystalline peaks of the silica and alumina compounds included muscovite (PDF 01-082-2723), quartz (PDF 01-070-7344), andesine (PDF 05-001-0869), and Amicite (PDF 00-033-1273). According to the XRF analysis in Table 1, the soil consisted of 68.90% SiO<sub>2</sub>, 13.50% Al<sub>2</sub>O<sub>3</sub>, 2.62% Fe<sub>2</sub>O<sub>3</sub>, and 1.94% CaO by weight with other minor compositions. The result of XRF showed that Shirasu soil is a silty sand according to containing 68.90% of SiO<sub>2</sub> [18] Additionally, its mineral composition has high quantity of volcanic glasses in and shows pozzolanic reaction [17].

## 2.2 Alkali-activating solution

The liquid alkaline activator was a mixture of sodium silicate (Na<sub>2</sub>SiO<sub>3</sub>) solution and sodium hydroxide (NaOH) varied concentration from 0.5 M to 9 M. The mixing ratio between Na<sub>2</sub>SiO<sub>3</sub> and NaOH was 1.0 wt%. The Na<sub>2</sub>SiO<sub>3</sub> solution (Nacalai Tesque, Japan) is composed of 61% H<sub>2</sub>O, 9% Na<sub>2</sub>O, and 30% SiO<sub>2</sub> with SiO<sub>2</sub> to Na<sub>2</sub>O ratio equal to 3.1 wt%. The pure 99 wt% NaOH pellets (Nacalai Tesque, Japan) were dissolved with distilled water to provide the NaOH solution of varied concentration from 0.5 M to 9 M.

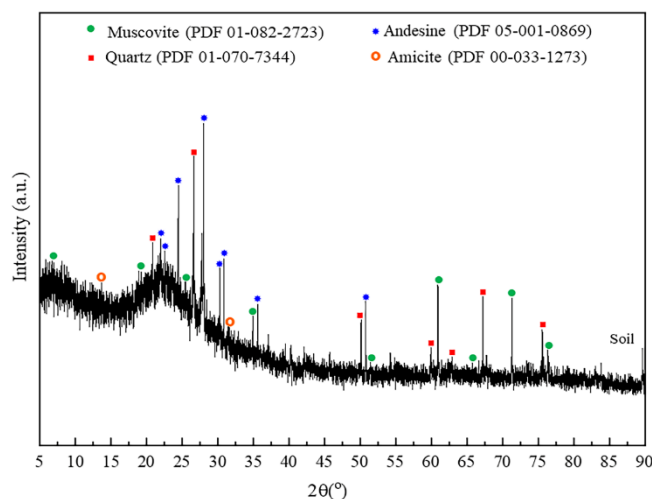


Figure 2. XRD pattern of Shirasu soil.

### 2.3 Geopolymer synthesis

In this study, the geopolymer paste was first prepared from a mixture of Shirasu soil and alkali-activating solution at a ratio of 4:3 by weight with sufficient water. For the mixing process, the soil and the activator were mixed together for 6 h using ball mill to achieve the homogenous geopolymer paste. Afterward, the resulting fresh pastes were poured into cylinder mold of 30 mm diameter size to produce cylindrical specimens. The molds were respectively heated in a microwave oven with varying power settings (200 W, 500 W, 700 W) and heating times (30 s, 60 s, 90 s, and 120 s). Previous research demonstrated that higher microwave powers enhanced the specimen temperatures and increased porosities of porous geopolymers [7]. Therefore, the geopolymer samples were suddenly measured the temperatures by an infrared thermal scanner after heating process. After temperature measurement, the hardened geopolymers were all demolded and cured in an oven at 80°C for 7 days for required curing age. Additionally, all geopolymer specimens were dried at 200°C for 24h to obtain the stiff specimens and then kept at room temperature after subjected to the high temperature until testing. Samples were named according to NaOH concentration (M), microwave power (W) and heating time (T).

### 2.4 Characterization

After mixing the alkaline with soil for 1 min, the slurry was heated, cured in a microwave oven following testing time and then immediately detected temperature by using an infrared thermal scanner. An average of three specimens were tested for each heating time. A detector based on direct X-ray detection technology of the chemical and mineral composition were determined using Rigaku analyzer. The X-ray diffraction patterns were collected using  $\text{Cu K}\alpha_1$  radiation and the diffraction patterns were scanned at 5° to 90° in  $2\theta$  at a rate of 2° per minute. The geopolymer specimens were measured and calculated apparent bulk density and water adsorption according to ASTM C373 [19]. Moreover, the morphological and microstructural features of geopolymer specimens were investigated by using Electron Microscope, JSM-6480LV, on gold-coated samples. The FTIR technique was used

to observe chemical properties. For FTIR measurement, hardened geopolymers were grounded and mixed with KBr at concentrations of 0.2 wt%. To evaluate the pores in sample microstructures, the Brunauer–Emmett–Teller (BET) method was used to measure the specific surface area of the sample. The pore size distributions were achieved from the  $\text{N}_2$  adsorption isotherms by using the Barrett–Joyner–Halenda (BJH) by means of nitrogen adsorption at 77 K and the isotherm corresponded to hysteresis loops [7].

## 3. Results and discussions

### 3.1 Effect of microwave powers and heating times on sample temperatures

Figure 3(a-d) depicts the temperature profiles of geopolymers via different microwave powers and NaOH concentrations in heating times of 30 s, 60 s, 90 s and 120 s, respectively. The liquid alkali-activating concentrations were from 0.5 M to 9 M. The results showed that the temperatures of all specimens increased by increasing heating times and microwave powers. Additionally, it was found that microwave powers of 200 W and 500 W were able to achieve solid geopolymer in a short period, especially with higher NaOH concentration. This may be because electromagnetic radiation induces dielectric heating by the absorption energy with polar molecules of  $\text{OH}^-$  and ionic conduction of  $\text{Na}^+$  [20]. The dipolar polarization and ionic conduction mechanisms occur when NaOH concentrations increase. Thus, the polar molecules absorb microwaves and oscillate back and forth resulting to heats up neighboring materials generate higher temperatures [7]. Additionally, the densification and vaporization of water in the geopolymer matrix was affected by microwave radiation. This is because the radiation accelerate the silica and alumina dissolution resulting to the geopolymer gel formation [10]. On the other hand, the mixtures at power of 200 W could not be hardened at all samples, especially at 30 s of heating times. This is because using 30 s of heating is not enough to accelerate the geopolymerization reaction. The slurries were still in gel phases.

### 3.2 Apparent Bulk density

To confirm the geopolymerization occurred, all hardened specimens after curing in an oven at 80°C for 24 h were soaked in water for 24 h and then measured the apparent bulk density. Figure 4 displays the apparent density of the geopolymers synthesized by different NaOH concentrations, microwave powers and heating times. The results showed that geopolymers synthesized at 200 W for 30 s in all NaOH concentrations were completely dissolved after soaking overnight as displayed in Figure 4(a). On the other hand, when heating at 200 W by increasing the heating time, it was found that the geopolymer slurry could be solidified and analyzed the apparent density as shown in Figure 4(b-c). Moreover, the geopolymers can be stable in shape by heating at 200 W, 500 W and 700 W for 120 s as shown in Figure 4(d). It can be seen that the apparent bulk density decreases by increasing the NaOH concentration. This postulate reason is because when the NaOH concentration increase, microwave energy can be transformed into heat and achieve the thermal affects to dissolved charged particles  $\text{Na}^+$

and  $\text{OH}^-$  ions, cause materials to heat up immediately [21]. Therefore, the strong alkali ions rapidly enhanced the temperature. Afterward, the bubbles from water evaporation occurred and created in the bulk porous structure resulted in decreasing the apparent bulk density [7]. The dissolution ability was affected by concentration of NaOH solution as the higher concentration provided sufficient  $\text{Na}^+$  and  $\text{OH}^-$  ions led to accelerate the condensation and denser [22]. Additionally, the pores reduced when the porosity decreased. This caused lower apparent bulk density, but higher water absorption [23,24].

### 3.3 Water absorption

Apart from the apparent density measurement, the hardened specimens were also tested the water adsorption. Figure 5(a-d) shows the water absorption of geopolymers after soaking in water for 24 h. The results indicated that the water adsorption was increased by increasing NaOH concentration. These results relate to the apparent bulk density. Hence, it can be concluded the water adsorption increases as the apparent bulk density decreases. Moreover, at heating time of 120 s, the geopolymer specimen synthesized with 0.5 M NaOH can be stable in shape when microwave powers at 200 W, 500 W, and 700 W were operated. Hence, the heating time of microwave power at 120 s was suitable for porous geopolymer synthesis at low alkaline concentration of 0.5 M NaOH as alkaline activator. Additionally, the water adsorption was increased from 20% to 45% in the case of heating at 700 W for 120 s. It indicated that there were more open pores in the geopolymer specimens related to increase of the water adsorption values.

### 3.4 IR spectrum

To observe the details of the vibrational transitions and the chemical bonding changes in molecular level, the hardened specimens were analyzed using infrared spectra. Figure 6 depicts the FT-IR spectra of the original soil and geopolymers. The notably characteristic bands of soil as aluminosilicate are at  $480\text{ cm}^{-1}$  and  $1,100\text{ cm}^{-1}$  which are the bending vibrations and asymmetric stretching of the Si–O–Si bonds, respectively [25]. The Si–O–Si was influenced by crystalline matrix components of quartz which indicated the presence of tetrahedral  $\text{SiO}_2$ . After microwave curing, the intensity of the peaks was apparently decreased and shifted to a lower wavenumber in each geopolymer spectrum. This shift indicates that the microwave curing can accelerate the geopolymerization reaction. A strong tendency was observed in the case of higher NaOH concentration. It is noteworthy that the intensity of the asymmetric stretching of the Si–O–Si peaks was shifted from  $1,100\text{ cm}^{-1}$  to a lower wavenumber at  $960\text{ cm}^{-1}$ . This phenomenon represents the dissolution, condensation, and reorganization. As known, the peak near  $960\text{ cm}^{-1}$  was represented the form of the Si–O–Si and Si–O–Al stretching vibrations in newly formed geopolymer gels [26]. Another band was represented the occurrence of Si–O–Si bonds at  $676\text{ cm}^{-1}$  [27]. Moreover, the occurrence of significant broad bands was detected at around  $3470\text{ cm}^{-1}$  and  $1650\text{ cm}^{-1}$  for O–H stretching ( $-\text{OH}$ ), and O–H bending ( $\text{H}-\text{O}-\text{H}$ ), respectively. However, in case of high NaOH concentration, the band of carbonate compound was found at  $1420\text{ cm}^{-1}$ . The formation of O–C–O in carbonate compounds occurred because of carbonation reaction [28].

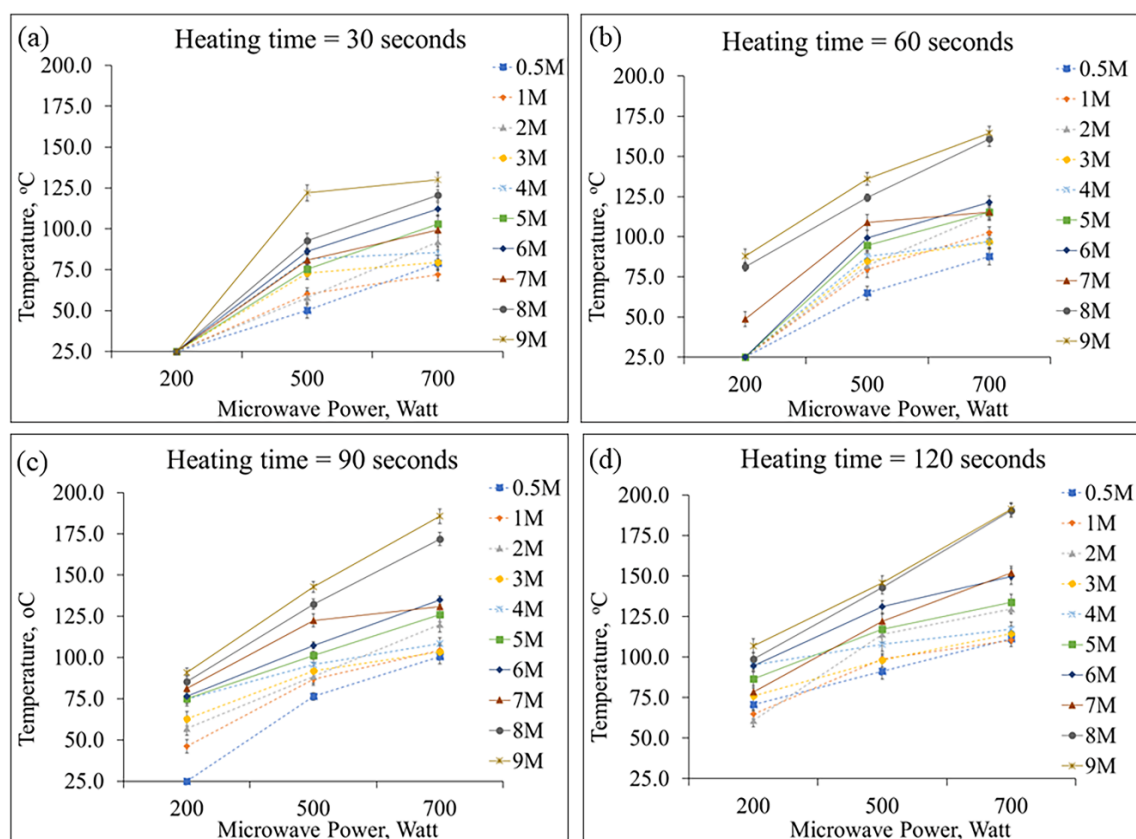


Figure 3. Temperature profiles of geopolymer specimens.

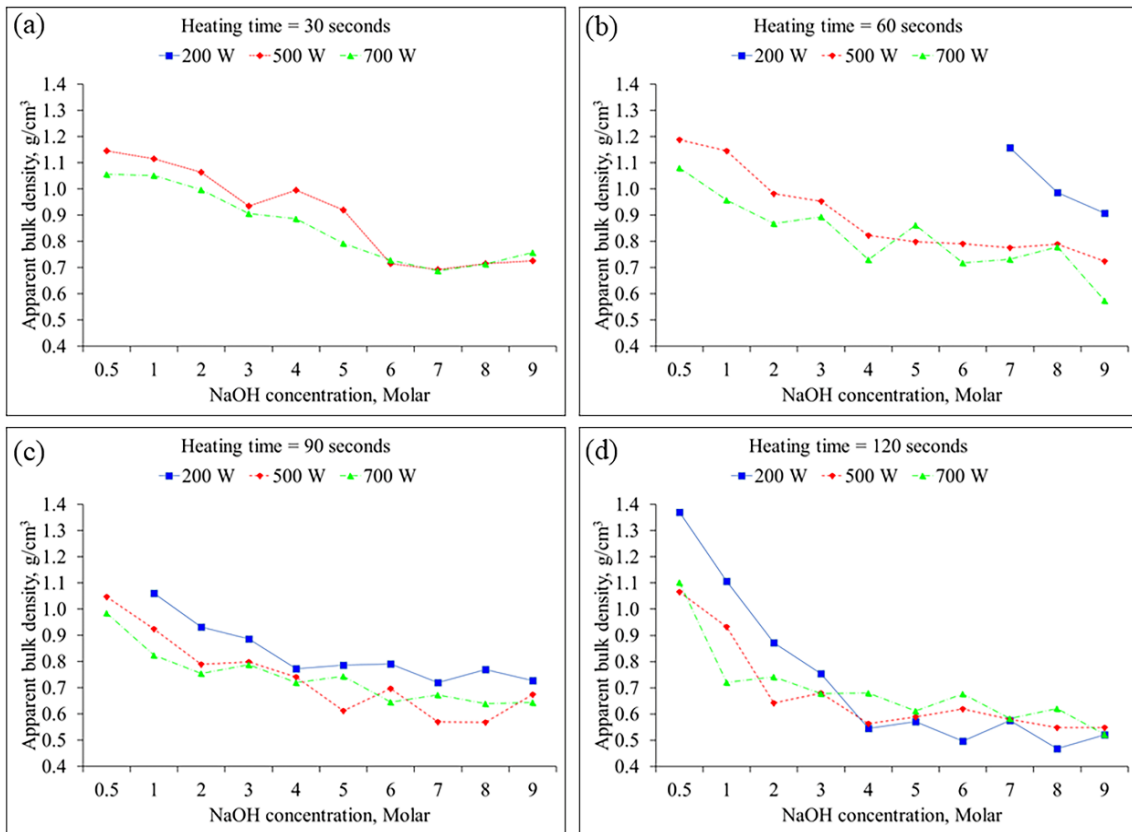


Figure 4. Apparent bulk density of geopolymers.

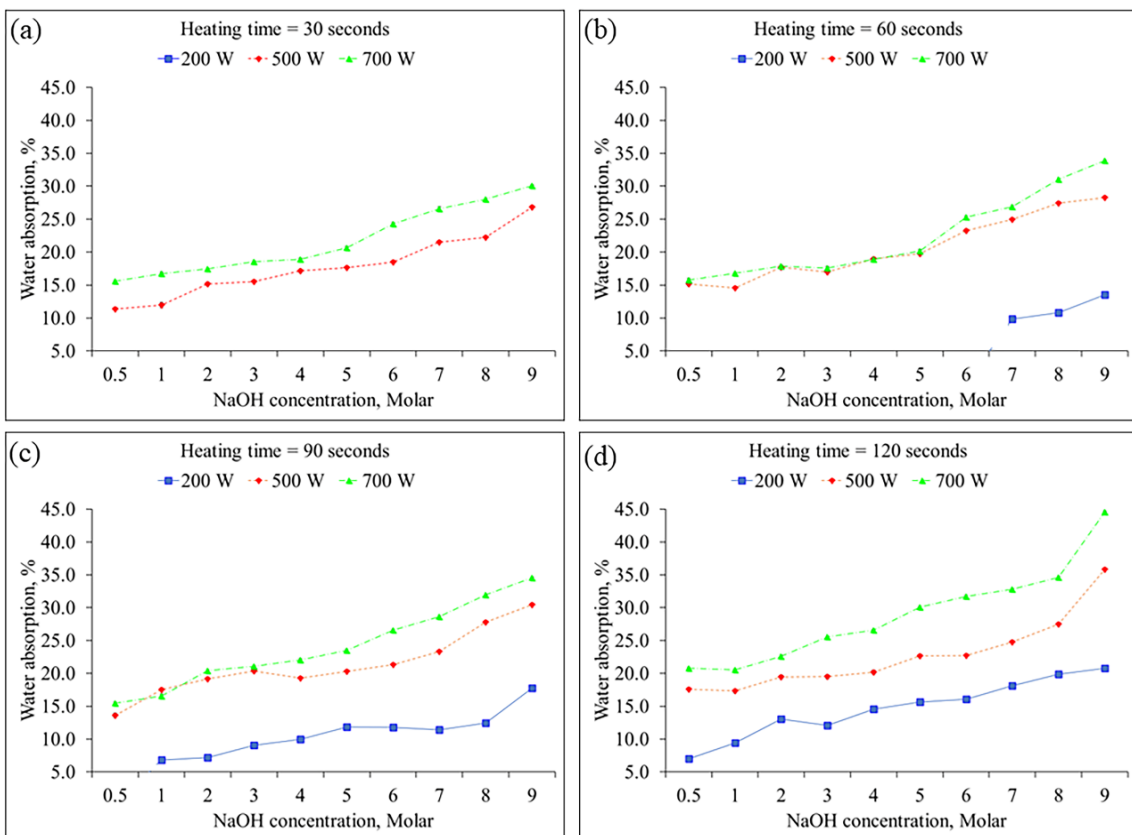
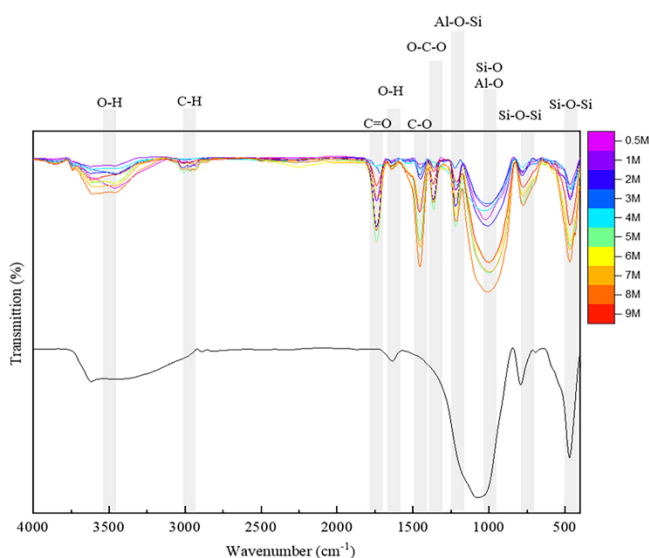


Figure 5. Water absorption of geopolymers.



**Figure 6.** IR spectra of geopolymer specimens with different heating time using microwave power at 700 W for 120 s.

### 3.5 SEM/EDS micrograph

Scanning electron microscopy (SEM) is displayed in Figure 7. According to Figure 7(a), it demonstrated that the soil particles have a mainly crystalline shape comprising different particle sizes. Moreover, the porous geopolymers synthesized by 1 M, 4 M, and 9 M NaOH at 700 W for 120 s were studied as displayed in Figure 7(b-d), respectively. SEM micrograph showed that not only porous structure was seen similarly in all samples of the matrix, but raw particles also remained in the geopolymer matrix. SEM results revealed that at 1.0 M NaOH, it was found unreacted particles of the soil. On the other hand, at 9 M NaOH, there were less unreacted particles. This is because increasing sodium hydroxide enhance due to a higher rate of polymerization [29]. In addition, in higher NaOH concentration, the denser structure appeared in the geopolymer matrices confirming that improved geopolymerization was responsible for increased NaOH concentration. At lower NaOH concentration, smaller porous was observed in the geopolymer matrices. After increasing NaOH concentration, the texture of the matrices was more porous and larger size of the pore. Hence, from these results, it can be confirmed that the high silica natural soil can be synthesized as a porous geopolymers using microwave radiation.

Basically, the geopolymer formation includes the dissolution, the hydrolysis, and the oligomerization process in an alkaline solution. Sodium and silicon ions are responsible for chemistry and physical properties of the geopolymers [30]. Therefore, it is vital to observe the effect of Si/Al ratio on micromorphology. To observe the chemical composition of porous geopolymers, the energy-dispersive X-ray spectroscopy (EDS) was performed to analyze the chemical element of samples synthesized with 1 M, 4 M and 9 M NaOH at 700 W for 120 s. The intensity of the element is shown in Figure 8. The higher

NaOH concentration caused the sodium atoms to slightly enhance from 6.43% to 20.98% by weight. Similarly, the aluminum atoms slightly increase 5.86% to 7.56% by weight. However, the silicon atoms are insignificant to be increased. This may be because the soil has a high crystalline structure. relating to difficult dissolution. Additionally, the Si/Al ratio of geopolymers activated 1 M, 4 M and 9 M were 5.40, 4.77, and 2.78, respectively. It can be seen from Figure 8 that the geopolymer activated by 9 M NaOH provided the highest geopolymer products in the matrix with the molar ratios in the range Si/Al < 3.3 as shown in previous study [31,32] Moreover, the Na/Al ratio is responsible for presenting the characteristic strength of the material [33]. According to Figure 8, the Na/Al ratio of geopolymer specimen activated by 1 M NaOH was 1.10 which provided higher apparent bulk density and deteriorated the strength because of alkali concentration limit as previous research [34]. Therefore, the higher NaOH concentration could provide the higher strength related to lower porosity because of sufficient Na<sup>+</sup> and OH<sup>-</sup> contents [22].

### 3.6 Nitrogen adsorption–desorption analysis

Nitrogen adsorption–desorption analysis was performed to evaluate the geopolymer matrix further. Figure 9(a-b) displays the nitrogen adsorption-desorption isotherm of the geopolymer samples by heating at 700 W for (a) 120 s and (b) 60 s. The results were calculated by the Barrett–Joyner–Halenda (BJH) of capillary condensation of the mesopores. From Figure 9(a), the results showed that when the NaOH concentration was increased from 1 M to 4 M, the quantity of the adsorbed nitrogen was enhanced. This phenomenon relates to the apparent bulk density of geopolymers. Even if the apparent bulk density of geopolymer activated by 1 M NaOH was higher than the samples activated by 4 M NaOH, the water absorption of the 1 M NaOH samples was lower than the 4 M NaOH samples. This indicates that the open pore volumes of the 4 M NaOH samples geopolymer were higher than the 1 M NaOH samples. Therefore, the values of the nitrogen adsorption was higher when the NaOH concentration increased. On the other hand, after NaOH reached 9 M, the nitrogen adsorption reduced with the increment of NaOH concentration. This implies that the surface area of geopolymers was reduced if the concentration of NaOH became higher because the higher NaOH concentration can immediately accelerate the geopolymerization provided a dense structure of the geopolymer matrix. Additionally, according to Figure 9(b), it found that the nitrogen adsorption-desorption of geopolymers activated at 60 s was lower compared to the samples were heated at 120 s. This may be because the amount of surface area was decreased. When the geopolymer slurry was heated over a longer period, the more bubbles and porous occurred related to achieve higher porosity and surface area. On the other hand, the shorter curing time had a tendency on less porosity and surface area. Hence, the quantity of N<sub>2</sub> adsorption-desorption was lower. It can be concluded that the porosity and surface area of porous geopolymers depend on the heating time of microwave radiation.

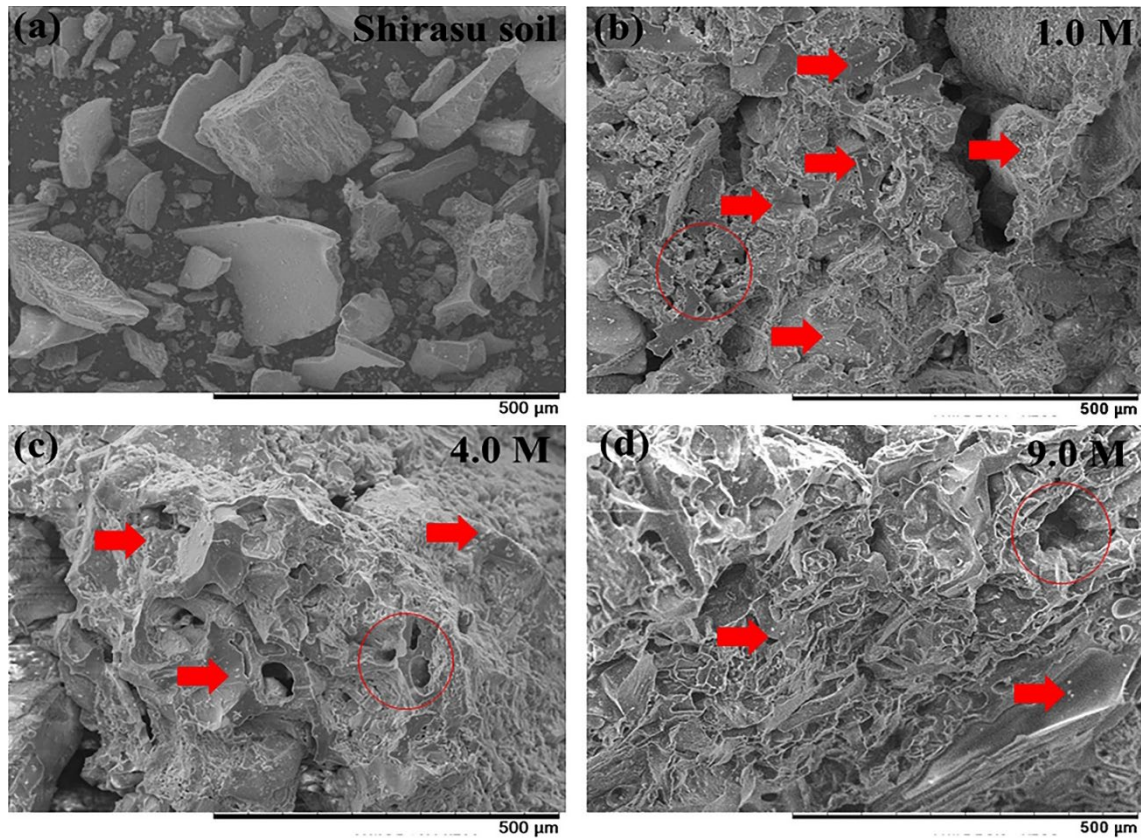


Figure 7. SEM image of Shirasu soil (a), and porous geopolymers (b-d).

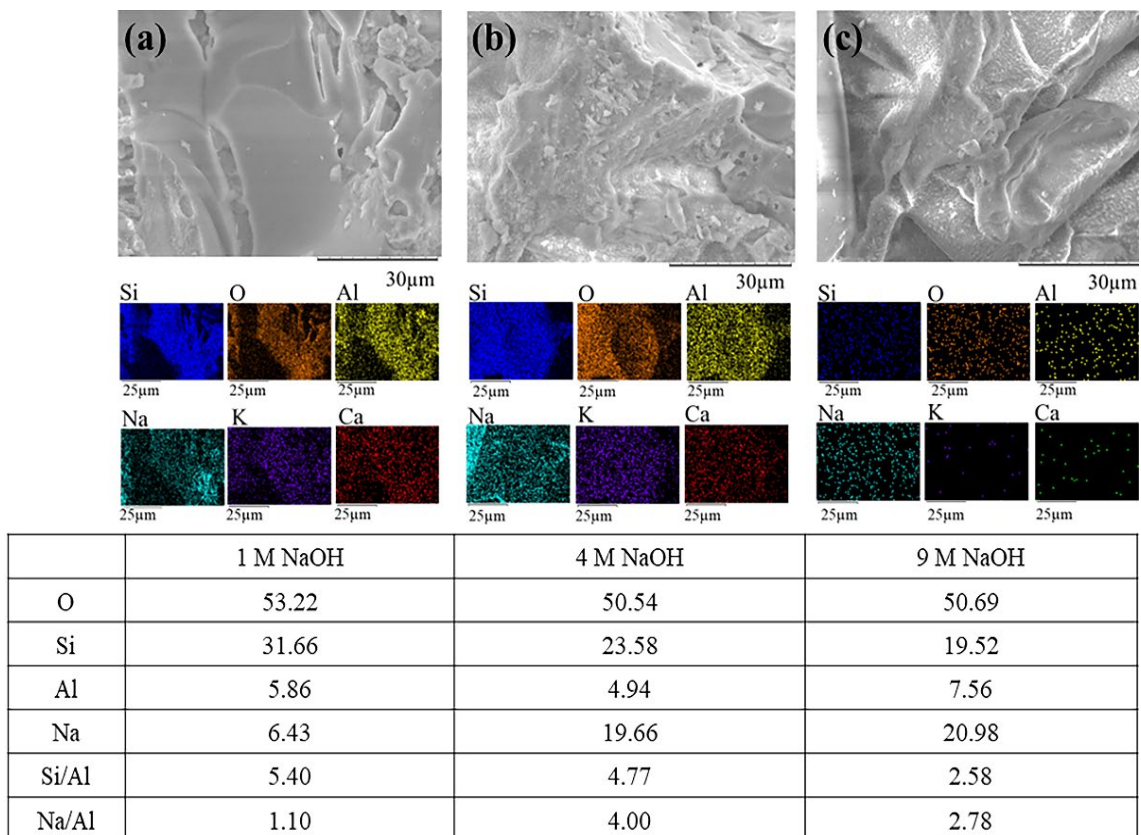


Figure 8. Elemental analysis with EDS.

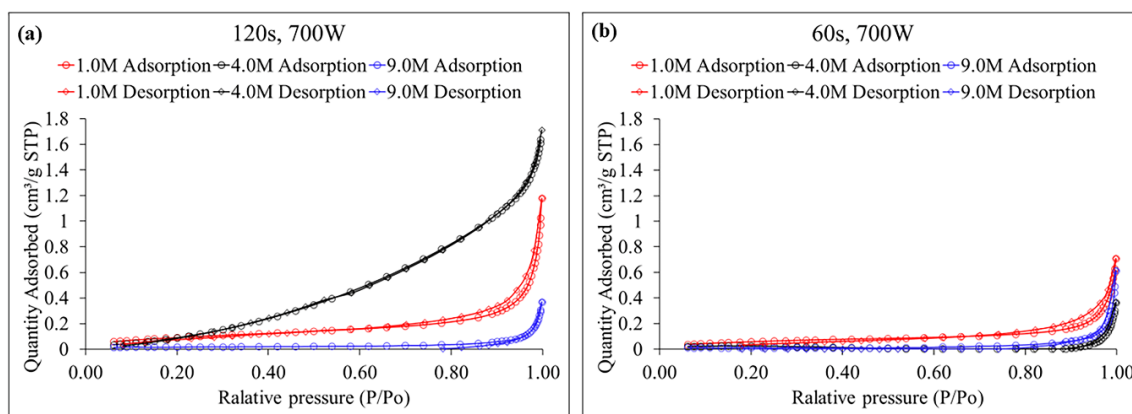


Figure 9. Nitrogen adsorption-desorption isotherm of geopolymers at 700W for (a)120s and (b)60s.

## 4. Conclusions

This paper studied the effects of microwave synthesizing porous geopolymers based high silica natural soil. A comparison of different microwave power, heating time and alkaline concentration were examined. Based on the results and discussion, the following significant conclusions can be drawn.

(1) Heating time of microwave curing of high silica natural soil based geopolymer was effective to porous geopolymers by higher NaOH concentrations. The higher NaOH concentration, microwave power and heating time were strongly supported the more porosity in geopolymer matrix.

(2) Increasing the microwave radiation power can promote and accelerate the geopolymerization reaction, has an impact on geopolymer durability in shape.

(3) Extending the microwave curing time promotes the higher nitrogen adsorption-desorption isotherm. However, over-time microwave curing shows a denser of geopolymer matrix which has negative effect in porous material application.

Overall, porous geopolymers were successfully fabricated through microwave curing method. This method can efficiently promote and accelerate the geopolymerization reaction of high silica natural soil as raw material. Based on the results, the porous geopolymers could be adapted to widely valuable applications, such as filtration, adsorption, and thermal insulation in which dense solid materials are not suitable. Additionally, they have been considered to be light weight porous materials, therefore, they could be adapted to remove contaminants of adsorbing organic dyes, heavy metal ions and of adjusting the pH. Further work should explore the potential applications, such as CO<sub>2</sub> or NO<sub>x</sub> capture and the adsorption of toxic contaminants in the field of wastewater treatment.

## Acknowledgements

This work was supported by CU Graduate School Thesis Grant, the 100th Anniversary Chulalongkorn University Fund for Doctoral Scholarship of Chulalongkorn University, the Overseas Research Experience Scholarship for Graduate Student by The Graduate School of Chulalongkorn University and another research fund by Global Academia-Industry Consortium for Collaborative Education (GAICCE).

## References

- [1] M. S. Muñoz-Villarreal, A. Manzano-Ramírez, S. Sampieri-Bulbarela, J. Ramón Gasca-Tirado, J. L. Reyes-Araiza, J. C. Rubio-Ávalos, J. J. Pérez-Bueno, L. M. Apatiga, A. Zaldivar-Cadena, and V. Amigó-Borrás, "The effect of temperature on the geopolymerization process of a metakaolin-based geopolymer," *Materials Letters*, vol. 65, no. 6, pp. 995-998, 2011.
- [2] N. Ranjbar, C. Kuenzel, J. Spangenberg, and M. Mehrli, "Hardening evolution of geopolymers from setting to equilibrium: A review," *Cement and Concrete Composites*, vol. 114, p. 103729, 2020.
- [3] Q. Wan, F. Rao, S. Song, R. E. García, R. M. Estrella, C. L. Patiño, and Y. Zhang, "Geopolymerization reaction, microstructure and simulation of metakaolin-based geopolymers at extended Si/Al ratios," *Cement and Concrete Composites*, vol. 79, pp. 45-52, 2017.
- [4] X. Zhao, C. Liu, L. Zuo, L. Wang, Q. Zhu, and M. Wang, "Investigation into the effect of calcium on the existence form of geopolymerized gel product of fly ash based geopolymers," *Cement and Concrete Composites*, vol. 103, pp. 279-292, 2018.
- [5] R. Mohamed, R. Abd Razak, M. M. A. B. Abdullah, R. K. Shuib, Subaer, and J. Chaiprapa, "Geopolymerization of class C fly ash: Reaction kinetics, microstructure properties and compressive strength of early age," *Journal of Non-Crystalline Solids*, vol. 553, no. November 2020, p. 120519, 2021.
- [6] S. Prasanphan, S. Onutai, and N. Nawaukarathamant, "Influence of partial replacement of calcined red clay by gypsum-bonded casting investment waste on geopolymerization reaction of red clay-based geopolymer," *Heliyon*, p. 104908, 2021.
- [7] S. Onutai, S. Jiemsirilers, P. Thavorniti, and T. Kobayashi, "Fast microwave syntheses of fly ash based porous geopolymers in the presence of high alkali concentration," *Ceramics International*, vol. 42, no. 8, pp. 9866-9874, 2016.
- [8] J. Sun, W. Wang, and Q. Yue, "Review on microwave-matter interaction fundamentals and efficient microwave-associated heating strategies," *Materials (Basel)*, vol. 9, no. 4, 2016.
- [9] X. Guan, W. Luo, S. Liu, A. G. Hernandez, H. Do, and B. Li, "Ultra-high early strength fly ash-based geopolymer paste cured by microwave radiation," *Developments in the Built Environment*, vol. 14, no. March, p. 100139, 2023.

- [10] P. Chindaprasirt, U. Rattanasak, and S. Taebuanhuad, "Role of microwave radiation in curing the fly ash geopolymer," *Advanced Powder Technology*, vol. 24, no. 3, pp. 703-707, 2013.
- [11] H. Gao, L. Liao, Y. Liang, X. Tang, H. Liu, L. Mei, G. Lv, and L. Wang, "Improvement of durability of porous perlite geopolymer-based thermal insulation material under hot and humid environment," *Construction and Building Materials*, vol. 313, no. October, p. 125417, 2021.
- [12] Y. Ettahiri, L. Bouna, J. V. Hanna, A. Benlhachemi, H. L. Pilsforth, A. Bouddouch, and B. Bakiz, "Pyrophyllite clay-derived porous geopolymers for removal of methylene blue from aqueous solutions," *Materials Chemistry and Physics*, vol. 296, no. December 2022, p. 127281, 2023.
- [13] Y. Ettahiri, B. Bouargane, K. Fritah, B. Akhsassi, L. P'erez-Villarejo, A. Aziz, L. Bouna, A. Benlhachemi, and R. M. Novais, "A state-of-the-art review of recent advances in porous geopolymer: Applications in adsorption of inorganic and organic contaminants in water," *Construction and Building Materials*, vol. 395, no. May, 2023.
- [14] S. Mingming, Z. Hengze, L. Ye, and Z. Lingqi, "The adsorption properties of steel slag-based porous geopolymer for  $\text{Cu}^{2+}$  removal," *Minerals Engineering*, vol. 201, no. July, pp. 1-10, 2023.
- [15] P. He, Z. Guo, X. Zhang, T. Wang, W. Zheng, and D. Liu, "Development of sulfhydryl grafted hierarchical porous geopolymer for highly effective removal of Pb (II) from water," *Separation and Purification Technology*, vol. 334, no. 13, p. 125954, 2024.
- [16] Y. Wang, L. Liu, C. Ren, J. Ma, B. Shen, P. Zhao, and Z. Zhang, "A novel amine functionalized porous geopolymer spheres from municipal solid waste incineration fly ash for  $\text{CO}_2$  capture," *Journal of Environmental Management*, vol. 349, no. July 2023, p. 119540, 2024.
- [17] Q. Wang, P. Yan, J. Yang, and B. Zhang, "Influence of steel slag on mechanical properties and durability of concrete," *Construction and Building Materials*, vol. 47, no. 1, pp. 1414-1420, 2013.
- [18] USDA, "Chapter 3 Engineering Classification of Earth Materials," Part 631 National Engineering Handbook, no. January, p. 35, 2012.
- [19] A. Abed AL-Jabar, H. Al-Kaisy, and S. Ibrahim, "Investigating the effect of different parameters on physical properties of metakaolin-based geopolymers," *Journal of Engineering Technology*, vol. 40, no. 12, pp. 1-10, 2022.
- [20] Y. Sun, P. Zhang, J. Hu, B. Liu, J. Yang, S. Liang, K. Xiao, and H. Hou, "A review on microwave irradiation to the properties of geopolymers: Mechanisms and challenges," *Construction and Building Materials*, vol. 294, p. 123491, 2021.
- [21] N. A. Jaya, L. Yun-Ming, M. M. A. B. Abdullah, H. Cheng-Yong, and K. Hussin, "Effect of sodium hydroxide molarity on physical, mechanical and thermal conductivity of metakaolin geopolymers," *IOP Conference Series: Materials Science and Engineering*, vol. 343, no. 1, 2018.
- [22] H. T. Ng, C. Y. Heah, Y. M. Liew, and M. M. A. B. Abdullah, "The effect of various molarities of NaOH solution on fly ash geopolymer paste," *AIP Conference Proceedings*, vol. 2045, pp. 6-11, 2018.
- [23] J. Wang, L. Han, Z. Liu, and D. Wang, "Setting controlling of lithium slag-based geopolymer by activator and sodium tetraborate as a retarder and its effects on mortar properties," *Cement and Concrete Composites*, vol. 110, no. April, p. 103598, 2020.
- [24] M. Zerzouri, S. Alehyen, R. Hamzaoui, L. Ziyani, and A. Loukili, "Durability of Moroccan fly ash-based geopolymer binder," *Materials Letters*, vol. 304, no. April, p. 130673, 2021.
- [25] A. Hajimohammadi, J. L. Provis, and J. S. J. Van Deventer, "The effect of silica availability on the mechanism of geopolymerisation," *Cement and Concrete Research*, vol. 41, no. 3, pp. 210-216, 2011.
- [26] A. R. Alvee, R. Malinda, A. M. Akbar, R. D. Ashar, C. Rahmawati, T. Alomayri, A. Raza, and F. U. A. Shaikh., "Experimental study of the mechanical properties and microstructure of geopolymer paste containing nano-silica from agricultural waste and crystalline admixtures," *Case Studies in Construction Materials*, vol. 16, no. November 2021, p. e00792, 2022.
- [27] A. Karthik, K. Sudalaimani, C. T. Vijayakumar, and S. S. Saravanakumar, "Effect of bio-additives on physico-chemical properties of fly ash-ground granulated blast furnace slag based self cured geopolymer mortars," *Journal of Hazardous Materials*, vol. 361, no. May 2018, pp. 56-63, 2019.,
- [28] A. A. Aliabdo, A. E. M. Abd Elmoaty, and H. A. Salem, "Effect of water addition, plasticizer and alkaline solution constitution on fly ash based geopolymer concrete performance," *Construction and Building Materials*, vol. 121, pp. 694-703, 2016.
- [29] H. Wang, H. Wu, Z. Xing, R. Wang, and S. Dai, "The effect of various si/al, na/al molar ratios and free water on micro-morphology and macro-strength of metakaolin-based geopolymer," *Materials (Basel)*, vol. 14, no. 14, 2021.
- [30] N. Waijarean, S. Asavapisit, K. Sombatsompop, and K. MacKenzie, "The Effect of  $\text{SiO}_2/\text{Al}_2\text{O}_3$  ratios on the properties of geopolymers prepared from water treatment residue (WTR) in the presence of heavy metals," *GMSARN International Journal*, vol. 1, no. 1.78, p. 97, 2014.
- [31] Mustofa, and S. Pintowantoro, "The Effect of Si/Al ratio to compressive strength and water absorption of ferronickel," *International Seminar on Science and Technology*, pp. 167-172, 2016.
- [32] H. Castillo, H. Collado, T. Droguett, S. Sánchez, M. Vesely, P. Garrido, and S. Palma, "Factors affecting the compressive strength of geopolymers: A review," *Minerals*, vol. 11, no. 12, pp. 1-28, 2021.
- [33] M. Steveson, and K. Sagoe-Crentsil, "Relationships between composition, structure and strength of inorganic polymers : PPPart 2 Fly ash-derived inorganic polymers," *Journal of Materials Science*, vol. 40, no. 16, pp. 4247-4259, 2005.
- [34] T. Kovářík, and J. Hájek, "Porous geopolymers: Processing routes and properties," *IOP Conference Series: Materials Science and Engineering*, vol. 613, no. 1, 2019.
- [35] C. Bai, and P. Colombo, "High-porosity geopolymer membrane supports by peroxide route with the addition of egg white as surfactant," *Ceramics International*, vol. 43, no. 2, pp. 2267-2273, 2017.

- [36] Y. G. Adewuyi, "Recent advances in fly-ash-based geopolymers: Potential on the utilization for sustainable environmental remediation," *ACS Omega*, vol. 6, no. 24, pp. 15532-15542, 2021.
- [37] Z. Guo, and C. Zhou, "Recent advances in ink-based additive manufacturing for porous structures," *Additive Manufacturing*, vol. 48, no. PB, p. 102405, 2021.
- [38] A. Graytee, J. G. Sanjayan, and A. Nazari, "Development of a high strength fly ash-based geopolymer in short time by using microwave curing," *Ceramics International*, vol. 44, no. 7, pp. 8216-8222, 2018.